Supporting Information

In situ construction of Sillén-Aurivillius layered perovskite based 0D/2D homologous Schottky junction for efficient piezo-photocatalytic activity

Jian Yang, Yali Xue, Chuang Han, Xiaorui Zhang, Ke Sa, Jin Jia, Hanlin Ye, Yujun Liang *

Engineering Research Center of Nano-Geomaterials of Ministry of Education, Faculty of Materials Science and Chemistry, China University of Geosciences, Wuhan 430074, China.

***Corresponding author:** Tel.: +86 27 67884814; fax: +86 27 67883733.

E-mail address: yujunliang@sohu.com (Yujun Liang)

1. Characterization methods

X-ray powder diffraction (XRD) patterns of the as-prepared samples were measured in the range 10-70° (2θ) on an X-ray diffractometer (D8-FOCUS, Bruker, Germany) operating with Cu Kα radiation (λ = 1.5418 Å). The morphologies of the as-prepared samples were analyzed by field emission scanning electron microscope (FE-SEM, SU8010, Hitachi, Japan) and transmission electron microscope (TEM, Tecnai G2 T20, FEI, America). Meanwhile, the energy-dispersive X-ray spectroscopy (EDS) spectra and elemental mapping images were recorded on an EDAX Genesis, which was attached to the FE-SEM. X-ray photoelectron spectroscopy (XPS) data were acquired on a Thermo Fisher Scientific equipped with an Al Kα as the excitation source. The UV-vis diffuse reflectance spectra (DRS) were performed on an UV-2550PC spectrophotometer (Shimadzu Corporation, Japan). The photoluminescence (PL) spectra were conducted on a fluorescence spectrometer (Fluoromax-4P, Horiba Jobin Yvon, New Jersey, USA), which was equipped with a 150 W xenon lamp as the excitation source. The photoluminescence decay curves were examined by a Fluorescence Spectrometer (FLS 920, Edinburgh Instruments, Livingston, UK). The degradation products were identified by High Performance Liquid Chromatography-Mass Spectrometry (HPLC-MS, Agilent 1290uplc/qtof6550-MS).

2. Electrochemical measurements

The photocurrent response spectroscopy, electrochemical impedance spectroscopy (EIS) and Mott-Schottky plots were collected on a standard three-electrode electrochemical analyzer (CHI760E, Shanghai). The as-prepared sample coated onto the FTO electrode was served as the working electrode, an Ag/AgCl (saturated KCl) as the reference electrode, and a Pt foil as the counter electrode. The Na_2SO_4 (0.1 M) solution and 300 W Xe lamp (with a 420 nm optical filter) were employed as electrolyte and light source, respectively. The working electrodes were prepared according to the following method: 5 mg of photocatalyst powder and 10 μL of Nafion solution (5 wt%) were dispersed into 1 mL ethanol, and then ultrasonic treatment for 1 h to prepare a homogeneous catalyst colloid. Finally, the resultant catalyst slurry was coated onto the precleaned FTO glass surface with an active area of ca. 1.00 cm × 1.00 cm and then dried in air.

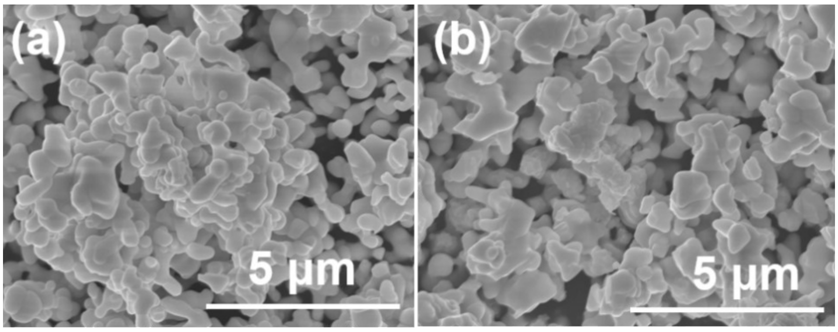

Fig. S1. SEM images of (a) BTOC-B and (b) BTOB-B.

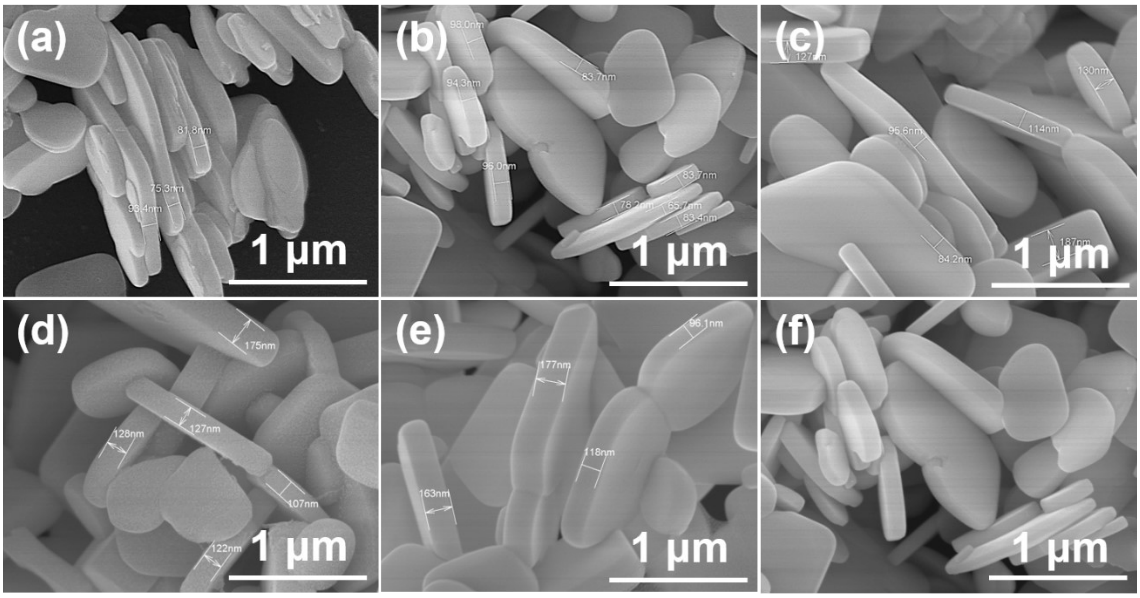

Fig. S2. SEM images of $Bi_4TaO_8Cl_xBr_{1-x}$ solid solution: (a) $x = 1$, (b) $x = 0.75$, (c, f) $x = 0.5$, (d) $x = 0.25$ and (e) $x = 0$.

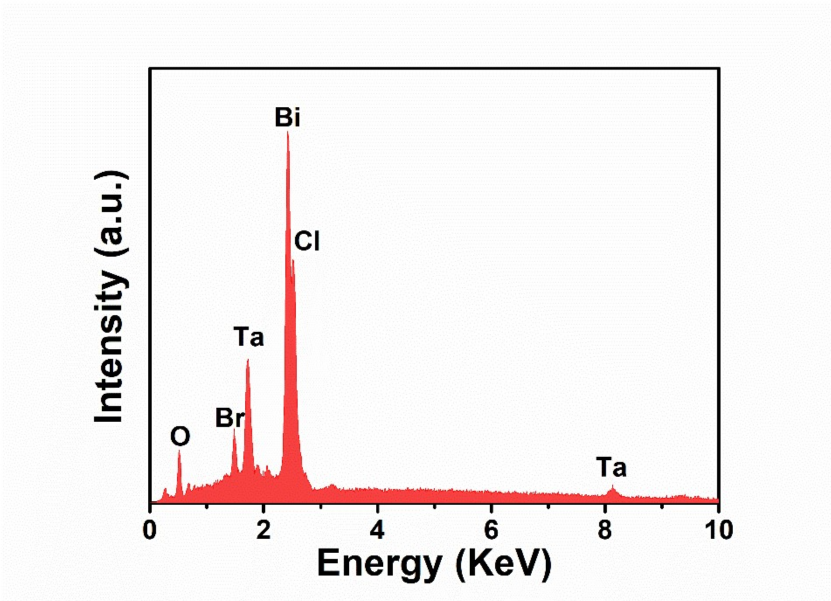

Fig. S3. EDS spectrum of Bi/BTOCB.

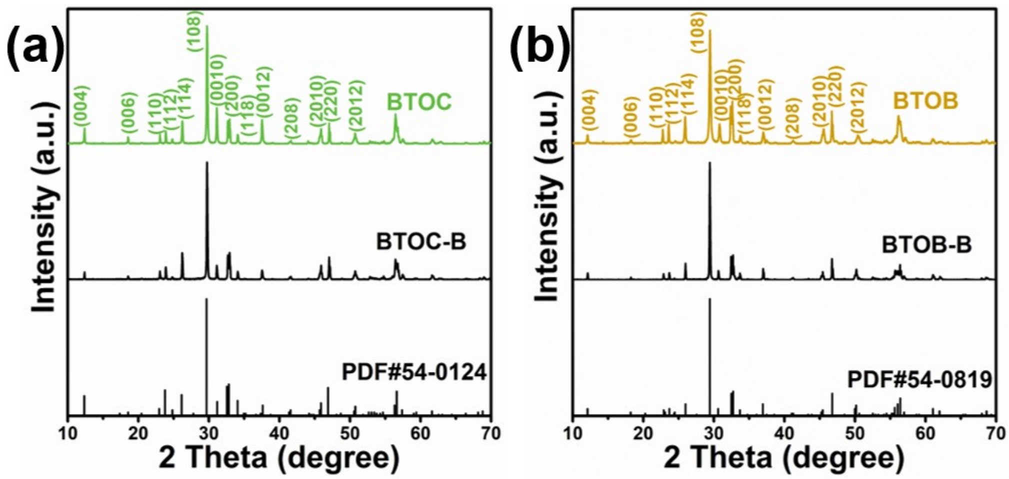

Fig. S4. XRD patterns of BTOC, BTOC-B, BTOB, and BTOB-B.

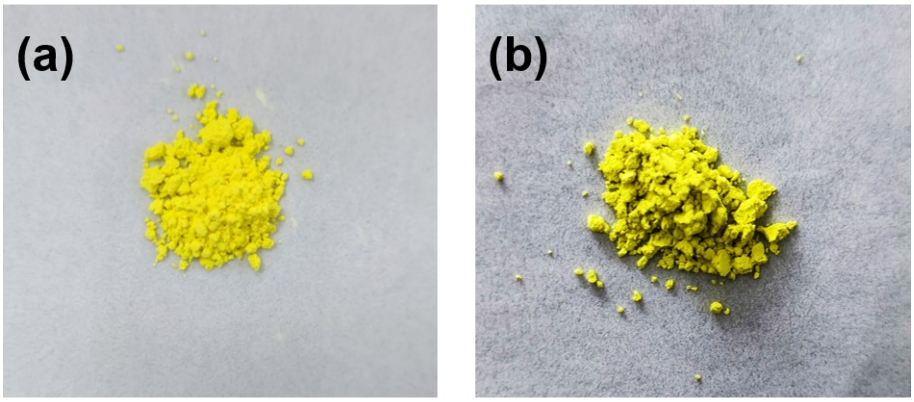

Fig. S5. The digital photographs of (a) BTOCB and (b) Bi/BTOCB.

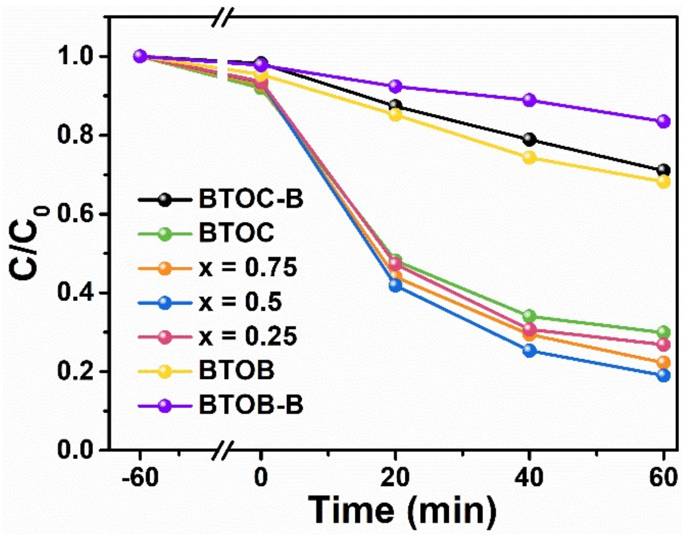

Fig. S6. The photocatalytic performance of the as-prepared samples for TC degradation.

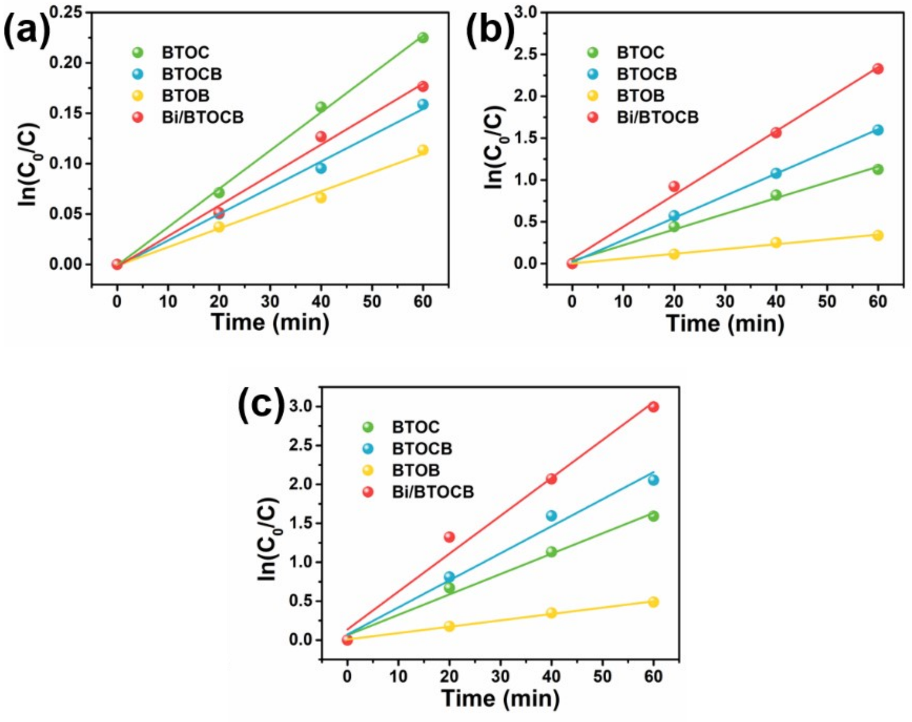

Fig. S7. The pseudo-first-order kinetics curves for degradation of TC over the as-prepared samples. (a) piezocatalytic, (b) photocatalytic, and (c) piezo-photocatalytic.

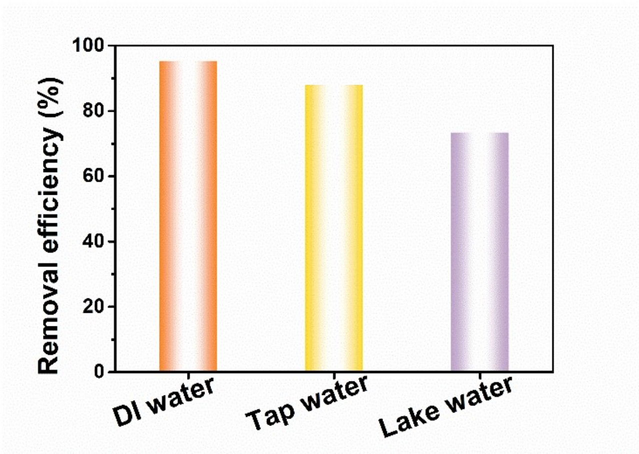

Fig. S8. Effect of different water bodies on the piezo-photodegradation of TC over Bi/BTOCB.

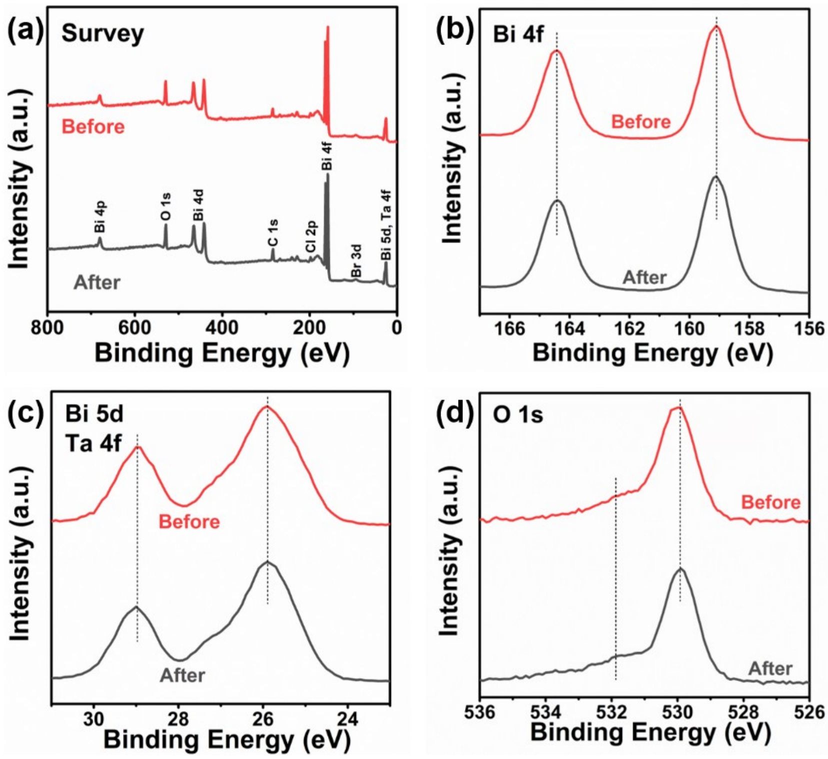

Fig. S9. XPS spectra before and after six cycles of Bi/BTOCB for piezo-photocatalytic reaction.

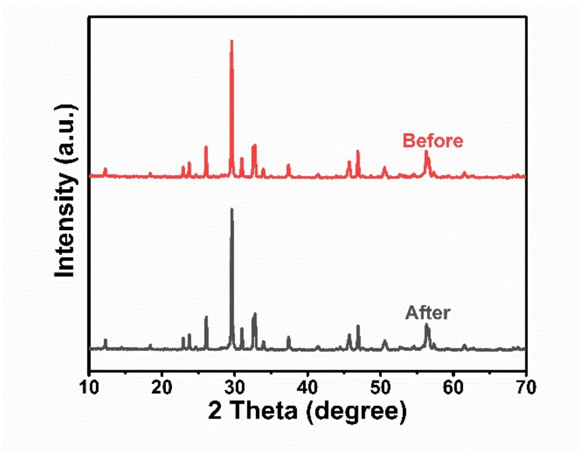

Fig. S10. XRD patterns before and after six cycles of Bi/BTOCB for piezo-photocatalytic reaction.

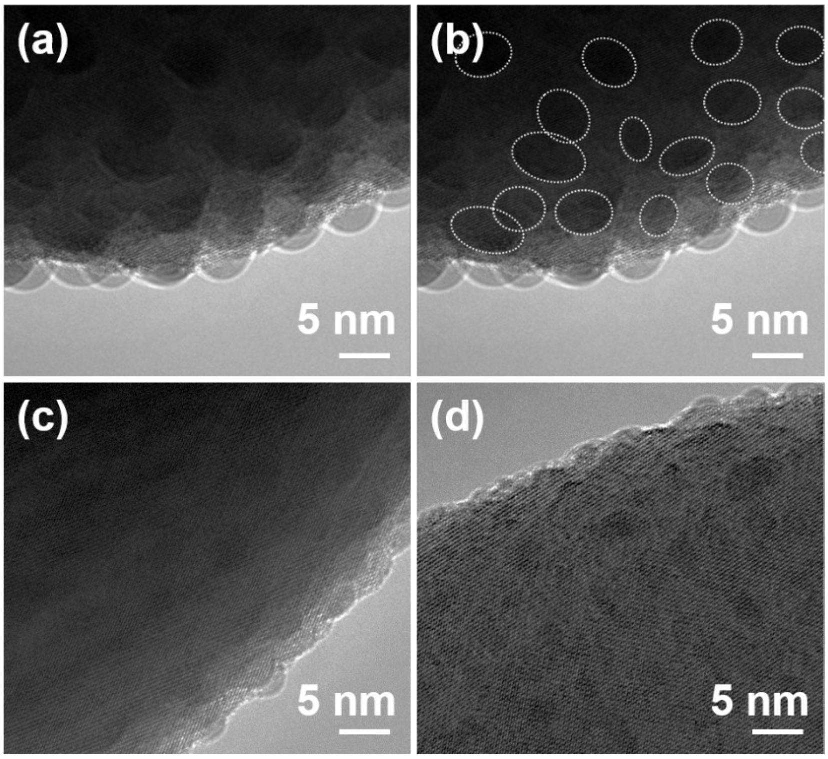

Fig. S11. TEM images before (a, b) and after (c, d) six cycles of Bi/BTOCB for piezo-photocatalytic reaction.

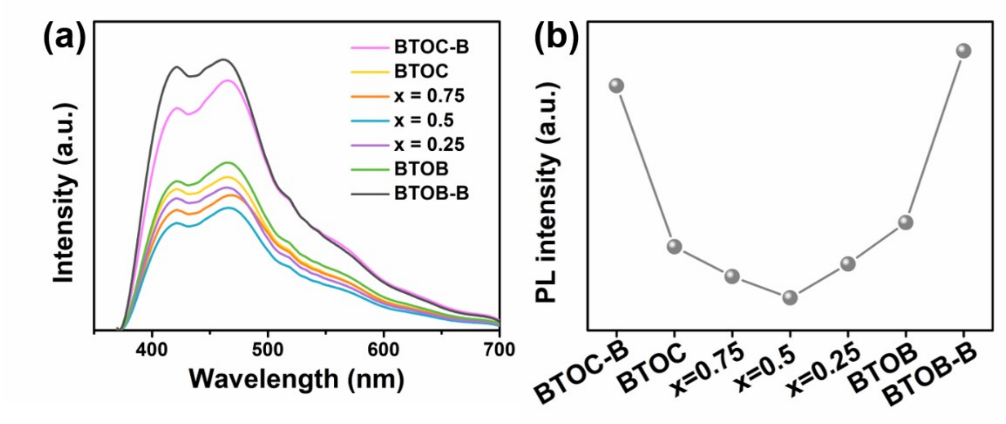

Fig. S12. PL spectra of as-prepared samples.

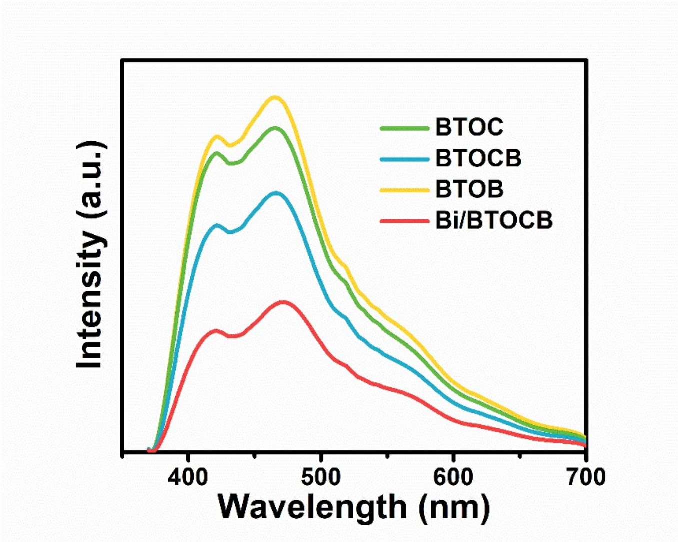

Fig. S13. PL spectra of BTOC, BTOCB, BTOB and Bi/BTOCB.

Table S1. Elemental composition of BTOCB (Atomic %) by EDS and XPS.

	Bi	Ta	O	Cl	Br
EDS	30.5	7.4	55.2	3.6	3.3
XPS	26.5	7.7	58.7	3.7	3.4

Table S2. Integrated areas of individuals XPS peaks of the Bi 4f from Bi/BTOCB.

	Peak 1	Peak 2	Peak 3	Peak 4
Binding Energy (eV)	164.44	163.29	159.13	157.95
Peak areas (a.u.)	135924.7	2787.026	174563.7	10251.96

Table S3. The rate constants k (min^{-1}) for TC degradation over the as-prepared samples.

Samples	Piezocatalysis	Photocatalysis	Piezo-photocatalysis
BTOC	0.0038	0.0188	0.0262
BTOCB	0.0026	0.0265	0.0347
BTOB	0.0019	0.0057	0.0082
Bi/BTOCB	0.0030	0.0381	0.0487

Table S4. Intermediates information in piezo-photocatalytic degradation of TC over Bi/BTOCB homologous Schottky junction.

No.	m/z	Molecular formula	Proposed Structure	
TC	445	$C_{22}H_{24}N_2O_8$	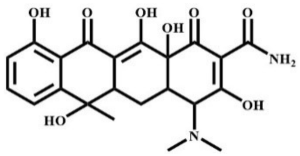	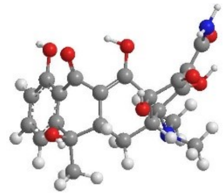
P1	475	$C_{22}H_{22}N_2O_{10}$	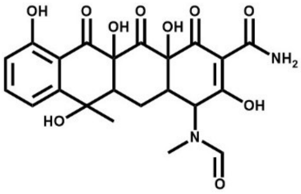	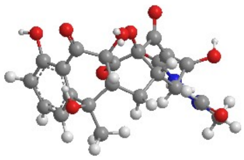
P2	419	$C_{20}H_{22}N_2O_8$	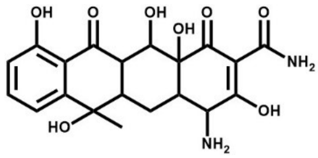	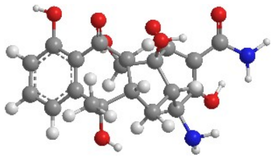
P3	429	$C_{20}H_{20}N_2O_9$	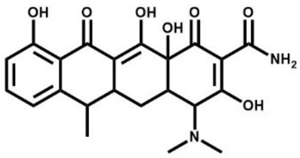	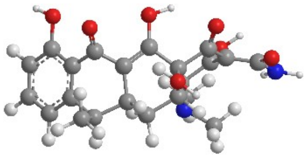
P4	410	$C_{22}H_{24}N_2O_7$	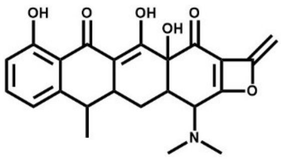	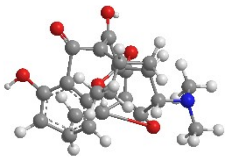
P5	376	$C_{19}H_{21}NO_7$	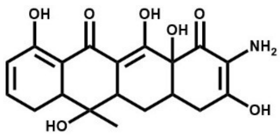	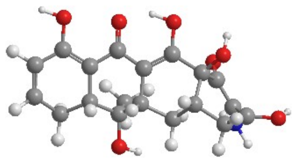
P6	449	$C_{21}H_{24}N_2O_9$	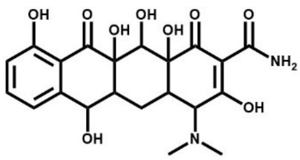	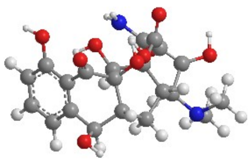
P7	371	$C_{18}H_{10}O_9$	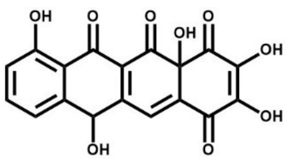	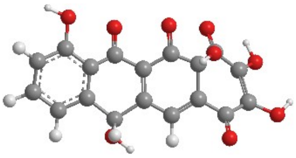

P8	353	$C_{19}H_{12}O_7$	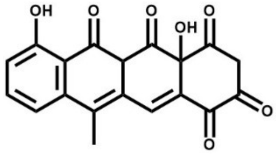	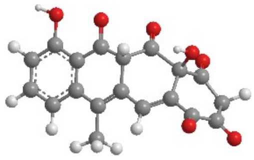
P9	149	$C_{10}H_{12}O$	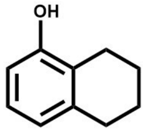	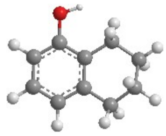
P10	107	C_7H_6O	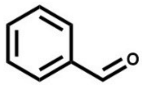	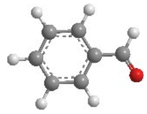
P11	89	$C_5H_{12}O$		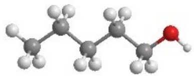
P12	223	$C_6H_6O_9$	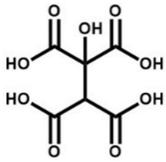	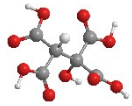

Table S5. Acute toxicological data of TC and its intermediates predicted by Toxicity Estimation Software Tool (T.E.S.T.).

No.	m/z	Fathead minnow LC_{50} (96 hr) mg/L	Daphnia magna LC_{50} (48 hr) mg/L
TC	445	0.90	8.70
P1	475	6.53	29.82
P2	419	1.02	7.76
P3	429	0.33	1.17
P4	410	9.77E-02	1.22
P5	376	2.74	3.05
P6	449	3.53	15.12
P7	371	8.39E-02	7.27
P8	353	0.51	13.07
P9	149	6.81	9.70
P10	107	13.87	15.90
P11	89	989.89	1444.12
P12	223	578.04	607.38

Table S6. Developmental toxicity and Mutagenicity data of TC and its intermediates predicted by Toxicity Estimation Software Tool (T.E.S.T.).

No.	m/z	Developmental Toxicity		Mutagenicity	
		Value	Result	Value	Result
TC	445	0.89	Developmental toxicant	0.56	Positive
P1	475	0.91	Developmental toxicant	0.59	Positive
P2	419	0.89	Developmental toxicant	0.65	Positive
P3	429	0.88	Developmental toxicant	0.78	Positive
P4	410	0.91	Developmental toxicant	0.44	Negative
P5	376	0.82	Developmental toxicant	0.64	Positive
P6	449	0.82	Developmental toxicant	0.51	Positive
P7	371	0.83	Developmental toxicant	0.62	Positive
P8	353	0.98	Developmental toxicant	0.56	Positive
P9	149	0.55	Developmental toxicant	0.08	Negative
P10	107	0.15	Developmental NON-toxicant	-0.04	Negative
P11	89	0.54	Developmental toxicant	0.35	Negative
P12	223	0.37	Developmental NON-toxicant	0.2	Negative